Int J Cardiovasc Imaging (2011) 27:619–627
DOI 10.1007/s10554-010-9705-1

ORIGINAL PAPER

Arterial supply of the sinoatrial node: a CT coronary angiographic study

Ersin Ozturk · Muzaffer Saglam · Ugur Bozlar · A. Kemal Sivrioglu · Bulent Karaman · Levent Onat · C. Cinar Basekim

Received: 31 May 2010 / Accepted: 10 September 2010 / Published online: 21 September 2010
© Springer Science+Business Media, B.V. 2010

Abstract We aimed to investigate the variances in especially the origin, course and termination of the sinoatrial node (SAN) artery in this study, using coronary CT angiography. The coronary CT angiography images of 251 patients (190 men and 61 women; age range, 20–82 years; mean age, 54.4 ± 13.6 years) were retrospectively analyzed. The SAN artery (arteries) in each case was named according to a special nomenclature with regard to their origin, course and termination. The sinoatrial node was being vascularized by a single artery in 241 (96%) cases and by two arteries in 10 (4%) cases. It was arising from RCA in 139 (55.4%) cases, from LCX in 99 (39.4%) cases, from the aorta in 2 (0.8%) cases, and from the bronchial artery in 1 (0.4%) case. The mean diameter of the SAN arteries was 2.3 mm. The mean distance between the origin of the SAN artery from RCA and the RCA ostium was 16.2 mm, from LCX and the origin of LCX was 19.3 mm. Frequency of the atrial branch was 35.9%. S-shaped SAN artery is determined in 51 (20.3%) cases. Coronary CT angiography is considerably effective in depicting the various vascularization types of SAN.

Keywords Heart · Coronary artery · Sinoatrial node artery · CT angiography

E. Ozturk · M. Saglam · A. Kemal Sivrioglu · C. Cinar Basekim
Department of Radiology, GATA Haydarpasa Teaching Hospital, 34668 Uskudar, Istanbul, Turkey

U. Bozlar (✉) · B. Karaman
Department of Radiology, Gulhane Military Medical Academy, 06018 Etlik, Ankara, Turkey
e-mail: ubozlar@yahoo.com

L. Onat
Department of Radiology, Florence Nightingale Hospital, 34668 Caglayan, Istanbul, Turkey

Introduction

The heart is one of the organs in the body in which vascular variations are frequently observed. Many coronary artery variations have been defined in previous studies [1–4]. The vast majority of these variations have been revealed as a result of studies performed by catheter angiography or anatomical dissection. Due to its high spatial and temporal resolution, catheter angiography is an effective method for demonstrating potential stenoses and dilations along the course and at the origin of the coronary arteries. However, the territories the heart perfuses may not be understood with certainty because the images are two-dimensional, and they do not display the structures in the heart except for the coronary arteries. In the anatomical studies, the paths of the vessels can be demonstrated very effectively, including very small branches, but the number of cases investigated in these studies is small.

Recent technological advances in CT technology have made it possible to demonstrate the coronary

arteries. The coronary CT angiography (CTA) allows submillimeter isotropic voxel imaging of coronary anatomy and also direct imaging of small coronary branches. Structures that have never been visible previously on CT, such as sinoatrial node (SAN) artery, can now be imaged as a part of the routine coronary artery studies. In studies using coronary CTA, it is possible to achieve substantially high case counts, to understand which vessels irrigate which part of the heart, and to visualize coronary artery and small branches with high resolution three-dimensional images.

Currently to the best of our knowledge, only a few published studies exist describing the use of coronary CT angiography for demonstrating the SAN artery [5, 6]. In this study, our aim was to demonstrate the variations in origin, course and termination of the SAN artery. We were motivated to evaluate the origin, course and termination of the SAN artery in such detail because this information is of great value for the cardiac surgeons and cardiologists who plan open cardiac surgery or angioplasty.

Materials and methods

Coronary CT angiograms of 269 cases with suspected or known coronary artery disease between July 2008 and October 2009 were reviewed retrospectively. A total of 18 cases were excluded from the study for various reasons: the presence of metal artifacts, such as surgical clips or pacemaker leads, leading to difficulty in evaluation, or inability to follow the coronary arterial path due to movement artifacts. A total of 251 cases were included in the study (190 men and 61 women; age range, 20–82 years; mean age, 54.4 ± 13.6 years). The study was approved by *our institutional review board.*

All CT examinations were performed using 64-section scanners (Brilliance-64, Phillips Medical Systems, Eindhoven, The Netherlands or LightSpeed VCT, GE Healthcare, Milwaukee, USA). A bolus of 80–120 ml iodine contrast agent, either iomeprol (Iomeron 400, Bracco, Milano, Italy) or iohexol (Omnipaque 350, GE Healthcare Ireland, Cork, Ireland), followed by 50 ml saline solution, was injected into an antecubital vein through an 18–20-gauge catheter at a flow rate of 6 ml/s using an automated power injector (Medrad Envision CT, Pittsburg, PA). Contrast agent administration was controlled by a bolus-tracking technique. A circular region-of-interest was selected in the descending aorta at the level of the carina, and image acquisition was started 5–6 s after the signal attenuation reached the predefined threshold of 150 HU. A beta-blocker (5–20 mg, Beloc ampul 5 mg/1 ml, AstraZeneca, Istanbul, Turkey) was given intravenously before the CTA if the heart rate was greater than 70 beats per minute. If no contraindication was present, 0.4 mg of sublingual nitroglycerin spray (Nitrolingual pump spray, Farma-Tek, Istanbul, Turkey) was administered just before scan initiation.

For the Brilliance-64 CT scanner, data was acquired using the following parameters: 64 × 0.625 mm detector collimation, 0.4 s gantry rotation time, pitch of 0.2–0.4 adapted to the heart rate, 120–140 kVp tube voltage, and 600–900 mA tube current. For the LightSpeed VCT scanner, data was acquired using the following parameters: 64 × 0.625 mm detector collimation, 0.35 s gantry rotation time, pitch of 0.2–0.4 adapted to the heart rate, 120 kVp tube voltage, and 300–700 mA tube current.

The radiation dose was changed between 12 and 34 mSv according to the scanned area. The scan area is from the carina to the inferior border of the heart (2 cm below the heart apex) in most patients. In patients who have undergone left or right internal mammarian artery grafts, the scan was started from the level of the clavicle.

Images were reconstructed at 35–85% of the cardiac cycle in increments of 5%. All images were interpreted by two radiologists on a three-dimensional workstation (EBW; Philips Medical Systems or Card IQ Xpress Pro, GE Healthcare) using multiplanar-reformatting (MPR), maximum intensity projection (MIP), and volume-rendering (VR) images.

The types of the SAN artery were determined by using a classification similar to that used by Ortale et al. [7] in his study. According to this classification, each SAN artery, except those originating from the aorta or the bronchial arteries, was classified into one of the following types: right or left (R or L) types, according to its origin from the RCA or LCX, respectively; subtypes L1, L2 or L3, according to its course, medial or posterior to the left auricle or, on the posterior surface of the left atrium, respectively; and R1 or R2, according to its course medial to the right auricle or on the posterior surface of the right

atrium, respectively (Fig. 1). Afterwards, each type was subdivided into a, b and c, according to the course of the terminal segment around the SVC being precaval, retrocaval or pericaval, respectively (Fig. 2).

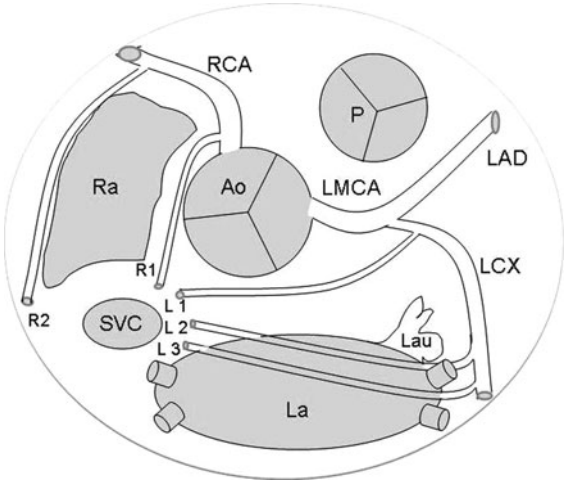

Fig. 1 The subtypes of the sinoatrial node artery with regard to its origin and course are seen in the illustration. *RCA* right coronary artery, *LMCA* left main coronary artery, *LAD* left anterior descending artery, *LCX* left circumflex artery, *Ao* aortic valves, *P* pulmonary valves, *Ra* right atrium, *La* left atrium, *Lau* left auricle, *SVC* superior vena cava

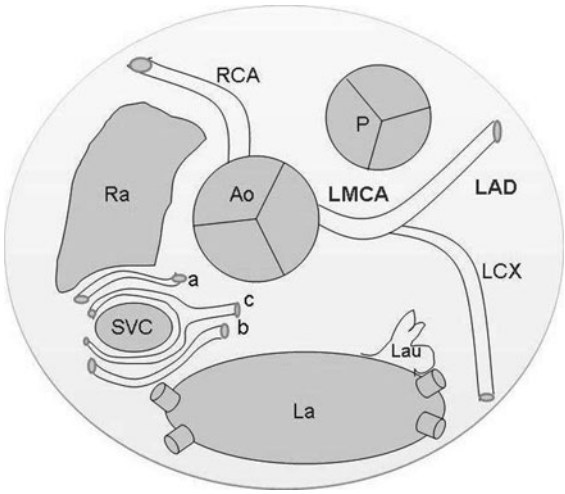

Fig. 2 The precaval (**a**), retrocaval (**b**) and pericaval (**c**) termination types of the sinoatrial node artery are demonstrated in the illustration. *RCA* right coronary artery, *LMCA* left main coronary artery, *LAD* left anterior descending artery, *LCX* left circumflex artery, *Ao* aortic valves, *P* pulmonary valves, *Ra* right atrium, *La* left atrium, *Lau* left auricle, *SVC* superior vena cava

We modified this classification by adding two more types as SAN arteries originating from aorta (A) and bronchial artery (B). Since these cases were a few in count, we could not divide these types into subtypes.

We evaluated the diameter of the SAN artery, the distance between RCA-LCX ostium and origin of the SAN artery, the distance between SAN artery and aortic root, number of the atrial branches, the distance between SAN artery and left auricle in the groove (for the L2 type), and probable atherosclerotic plaques in the SAN arteries. All the measurements were performed on axial images. We also evaluated the dominance of the coronary circulation in each case. The type of the SAN artery in each case was determined by two radiologists separately. In case of a discrepancy between the two radiologists' judgments, the final decision was made by consensus.

Statistical analyses were performed by the Independent Samples Test or the Pearson Chi-Square test.

Results

A total of 261 SAN arteries were detected in 251 cases (Table 1). The SAN was being supplied by a single artery in 241 (96%) cases and two arteries in 10 (4%) cases. The SAN was being fed by a single artery arising from RCA in 139 (*55.4%*) cases, from LCX in 99 (*39.4%*), from the aorta in 2 (0.8%), and from the bronchial artery in 1 (0.4%) case (Fig. 3a, b). Among the cases that are being fed by two separate branches, the SAN was being supplied by branches arising from RCA and LCX in 8 (*3.2%*) cases, from RCA and the bronchial artery in 1 (0.4%) case and, from LCX and the bronchial artery in 1 (0.4%) case. SAN artery arising from bronchial artery was observed in 3 (1.2%) cases.

Among the 251 cases, the circulation was right dominant in 199 (*79.3%*), left dominant in 37 (*14.7%*), and codominant in 15 (*6.0%*). No statistical relationship could be established between the dominance in the circulation and the origin of the SAN artery ($P = 0.33$).

When those arising from the aorta and bronchial artery and the R2 subtypes are excluded, the termination types in the remaining 253 SAN arteries was precaval in 91 (*36%*), retrocaval in 122 (*48.2%*), and pericaval in 40 (*15.8%*; Fig. 4). There was no

Table 1 Types of SAN artery and their frequencies, when all arteries are evaluated individually

Origin	Subtypes	No. of cases	%
R		148	56.7
	R1	145	55.6
	R1a	55	21.1
	R1b	68	26.1
	R1c	22	8.4
	R2	3	1.2
L		108	41.4
	L1	56	21.5
	L1a	21	8.0
	L1b	24	9.2
	L1c	11	4.2
	L2	51	19.5
	L2a	15	5.7
	L2b	29	11.1
	L2c	7	2.7
	L3	1	0.4
	L3a	–	–
	L3b	1	0.4
	L3c	–	–
A		2	0.8
B		3	1.2
Total		261	100

R right, *L* left, *R1* medial to the right auricle, *R1a* precaval, *R1b* retrocaval, *R1c* pericaval, *R2* on the posterior surface of the right atrium, *L1* medial to the left auricle, *L1a* precaval, *L1b* retrocaval, *L1c* pericaval, *L2* posterior to the left auricle, *L2a* precaval, *L2b* retrocaval, *L2c* pericaval, *L3* on the posterior surface of the left atrium, *L3a* precaval, *L3b* retrocaval, *L3c* pericaval, *A* aorta, *B* bronchial artery

statistically significant relationship between the origin of the SAN artery and the course of the terminal segment ($P = 0.49$).

The R1b type observed in 68 out of 261 SAN arteries (26.1%) was the most frequent type. The distribution of all SAN arteries with regard to their types is summarized in Table 1. R1b was also the type observed most frequently, when males and females were evaluated separately, within themselves. No statistically significant difference was observed between genders, with regard to the distribution of the types ($P = 0.912$).

The median diameter of 261 SAN arteries encountered in 251 cases was 2.26 mm. The widest diameter for a SAN artery was 3.6 mm, and the smallest was 1.3 mm. The mean diameter for the SAN artery was 2.29 mm in males and 2.16 mm in females. There was a statistically significant difference between men and women, with regard to the diameter of the SAN artery ($P = 0.021$). The mean diameters for the SAN arteries arising from RCA and LCX were 2.3 and 2.19 mm, respectively. The difference was statistically significant ($P = 0.017$). While the mean value for this diameter was 2.26 mm in the cases where the SAN is being fed by a single artery, it was 2.04 mm in those being fed by two arteries. The difference was statistically significant ($P = 0.011$).

The mean distance from the origin of 148 SAN arteries arising from RCA to RCA ostium was 16.2 mm. The longest distance measured was 62 mm. The SAN artery arose from RCA immediately at the level of ostium in one of the cases and this distance was

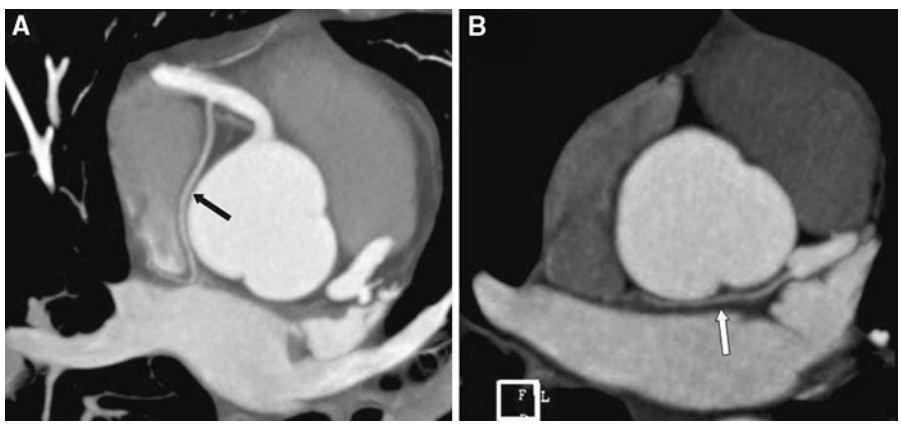

Fig. 3 **a** R1b subtype SAN artery arising from RCA (*black arrow*) is seen in the axial MIP view. **b** The SAN artery arising from LCX (*white arrow*) is seen in the axial MIP view

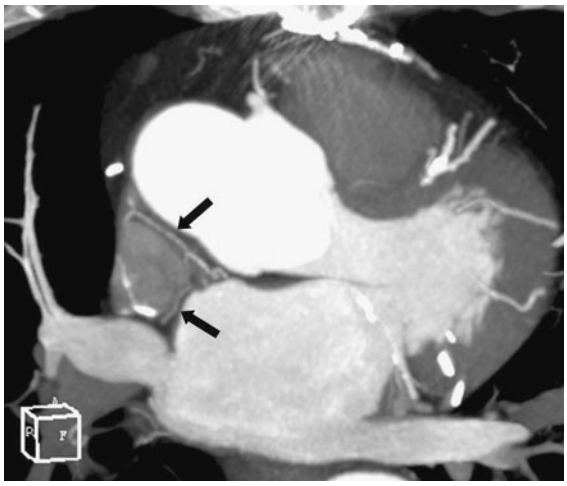

Fig. 4 SAN artery with a pericaval termination (c subtype) (*black arrows*) is seen in the MIP image

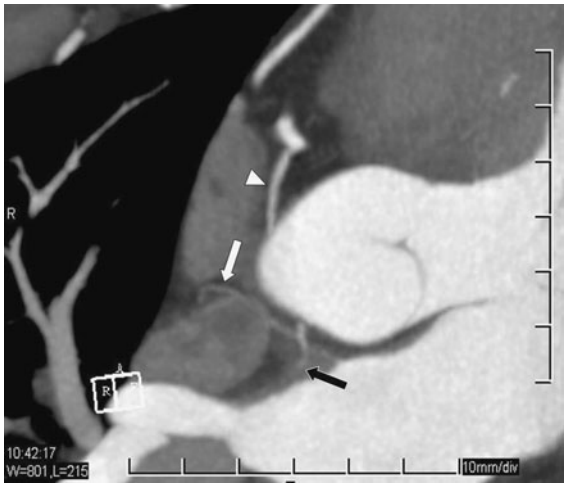

Fig. 5 R1a subtype SAN artery (*arrowhead*) with a precaval termination (*white arrow*) and an atrial branch (*black arrow*) are seen in the MIP image

accepted as zero. The mean distance from the origin of 108 SAN arteries arising from LCX to the origin of LCX was found to be 19.3 mm. The range for this distance was 2–66 mm.

The mean distance between aorta and R1 type SAN arteries that run medial to the right auricula was 0.88 mm. And the mean distance between aorta and L1 types which run medial to the left auricula was 1.92 mm.

Among the 251 cases, there was one single atrial branch in 87, and 2 atrial branches in 3 cases (Fig. 5). Atrial branch frequency was *35.9%*. The atrial branch was observed most frequently in the R1b type (29 cases).

The S-shaped SAN artery which is considered to be a variant of SAN artery arising from LCX was found in 51 cases (20.3%) out of 251 (Fig. 6a, b). S-shaped SAN artery frequency among the 108 SAN arteries arising from LCX was 47.2%. The mean diameter for S-shaped SAN arteries was 2.23 mm. The difference was not statistically significant, when this distance was compared with the mean diameter for all SAN arteries ($P = 0.613$). The mean for the shortest distance between S-shaped SAN arteries and left auricula was 2.41 mm.

An atherosclerotic plaque was identified in the SAN artery in 3 cases (1.2%) out of 251. When all coronary arteries were evaluated, coronary artery disease was present in 113 of the 251 (45%) cases.

Discussion

Several anatomic and angiographic studies have revealed some anatomical variations of the SAN artery [7–10]. However, there are just a few studies in the literature where the origin, course, and termination of the SAN artery have been investigated by coronary CTA [5, 6].

The frequencies found for the origin of the SAN artery in related studies, including the present study, are presented in Table 2. As can easily be observed, the closest values with our study were found in the study performed by Saremi et al. [5]. Interestingly, this study is one of the two studies performed before our study by multidetector CT (MDCT). The frequency for a SAN artery arising from LCA is reported to be between 10 and 33.7% in three different studies [11–13]. The difference between these studies and ours may be originating from ethnic differences between the study groups. Similarly, while triple SAN artery is reported with a frequency of 2 and 3.8% in two different studies [7, 14], we have not encountered a triple SAN artery in any of our cases. The SAN artery can rarely (1.7–3.5%) arise directly from aorta [15, 16]. We have spotted 2 (0.8%) SAN arteries arising from right sinus valsalva in our study. Non-coronary supply (SAN arteries arising from the aorta and the bronchial artery) was encountered in 5 out of 251 cases (2%); this rate has

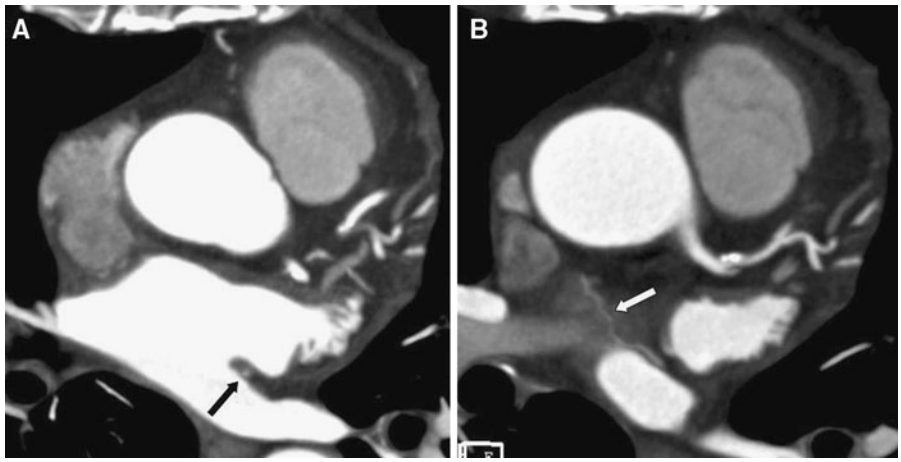

Fig. 6 S-shaped SAN artery arising from LCX and reaching the SAN after crossing between the left superior pulmonary vein and left atrial auricular (*black* and *white arrows*) is seen in the MIP images

been reported as 2 and 6.6% in two separate studies [7, 16].

SAN arteries reaching the SAN via a retrocaval or pericaval course can be surgically traumatized during superior transseptal incisions [17]. In a study performed by Saremi et al. [5], it was found that the terminal segment of the SAN artery reaches the SAN following one of these paths—retrocaval (47.5%), precaval (42.6%) or pericaval (9.9%). Yet in another study performed again by Saremi et al. [6], the same rates were found to be 64.7, 29.4 and 5.9%, respectively. In the study by Busquet et al. [18] these rates were found to be 36, 58, and 6%, respectively. Just like the former study, we have mostly encountered with retrocaval type termination. However, the pericaval type termination was found to be more frequent than the other two studies.

The frequencies found in our study for R1, R2, L1, L2 and L3 were 54.4, 1.2, 21.5, 19.5 and 0.4%, respectively. In the study performed by Ortale et al. [7], the same rates were found as 46, 4, 24, 16 and 4% respectively, which demonstrates a great similarity with ours. While far most of the SAN arteries (98%, when only the ones arising from RCA are taken into account) originating from RCA reach the SAN following a path medial to the auricula, only 51.9% of the ones originating from LCX reached the SAN after a course between aorta and left auricula (Fig. 7).

There are studies in the literature regarding the diameter of the SAN artery, which are performed on cadavers, or via catheter angiography or MDCT. However, the vessel diameters are found larger because of the use of sublingual nitroglycerin in the studies performed with MDCT. The mean diameters for SAN arteries are reported as 1.1 and 1.7 mm in two different cadaver studies [7, 19]. The mean diameter for SAN artery is found to be 2.26 in our study, and this value is higher than those above. Pejković et al. [8] have reported in a cadaver study over 150 hearts a mean diameter of 1.7 mm for SAN arteries arising from right side and 2.2 mm from the left side, while Saremi et al. have found 1.6 mm for the right-sided and 1.4 mm for the left [6]. Although the results of the measurements in our study are higher than those in both of the mentioned studies, the mean diameters of the SAN arteries arising from the right side were found to be wider than those arising from the left, similar with the study by Saremi et al. Statistically, the most striking findings in our study were related with the diameter of the SAN arteries. We have observed that the diameters of SAN arteries arising from the right side are wider than those from the left, and males have a wider SAN artery, when compared with those in females, and both findings were significant statistically. Similarly, the single SAN arteries had a statistically significantly wider diameter than those which are part of a dual vascularization.

S-shaped SAN artery is an anatomical variation of the SAN artery arising from LCX. After departure, it runs posteriorly between the left atrial appendage and the ostium of the left superior pulmonary vein and then anteriorly, close to the anterior wall of the left atrium

Table 2 The results found in the studies regarding the origin of the SAN artery

Study (reference no)	Single SAN artery (%)					Dual SAN artery (%)			Triple SAN Artery (%)
	RCA originated	LCX originated	LCA originated	Bronchial artery originated	Aorta originated	RCA-LCX originated	RCA-Bronchial artery originated	LCX-Bronchial artery originated	
Campbell [11]	52.6	13.7	33.7						
James [21]	55.0	45.0							
Romhilt et al. [22]	60.8	37.6				1.6			
Hadziselimovic [23]	60.0	40.0							
Bokeriya et al. [12]	61.4	28.6	10.0						
Caetano et al. [13]	58.0	30.0	12.0						
Busquet et al. [18]	66.0	30.0				4.0			
Sow et al. [24]	64.5	24.4				11.1			
Futami et al. [25]	73.4	3.3				23.3			
Kawashima et al. [14]	32.0	14.2				50.0			3.8
Ortale et al. [7]	50.0	44.0				4.0			2.0
Vieweg et al. [26]	53.0	35.0				11.0			
Saremi et al. [6]	65.7	27.4				5.9			
Saremi et al. [5]	54.5	40.6				4.9			
Current study	55.4	39.4		0.4	0.8	3.2	0.4	0.4	

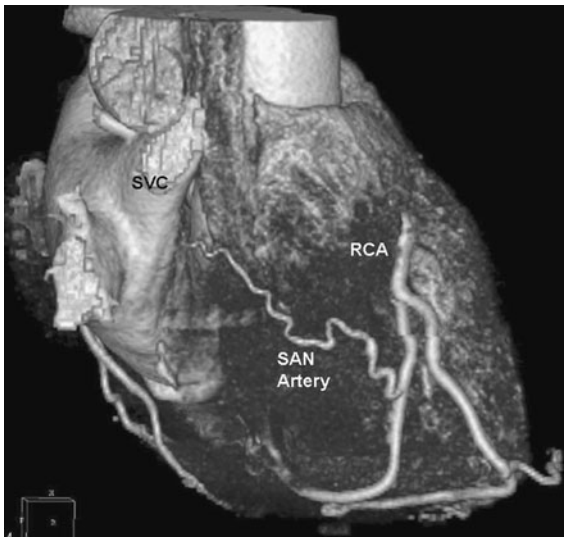

Fig. 7 R2 subtype SAN artery arising from RCA and reaching the SAN adjacent to the superior vena cava, after crossing from lateral side of the right atrium is seen in the VR image

[6]. Awareness for this variation is particularly important in cases where a surgical intervention and/or a catheter-based ablation at the left atrium is planned. S-shaped SAN artery frequency is reported in the literature as between 5.9 and 16% [5–7, 20]. We have spotted an S-shaped SAN artery in 20.3% of our cases. When the SAN arteries arising from left side are taken into account, 47.2% were in this type. Saremi et al. [6] have reported that the mean diameter of the S-shaped SAN arteries is 2.1 mm and this diameter is wider than those of other types of SAN artery. The mean diameter for S-shaped SAN arteries is found as 2.2 mm and the difference from those of other types of SAN arteries was not statistically significant.

In conclusion, *MDCT* depiction of the variable arterial blood supply to the SAN may provide valuable information prior to any planned surgical or catheter-based interventional cardiac procedures in patients. Coronary CTA is an effective imaging technique for identifying different irrigational patterns of the SAN.

References

1. Angelini P (1989) Normal and anomalous coronary arteries: definitions and classification. Am Heart J 117:418–434
2. Basso C, Maron BJ, Corrado D, Thiene G (2000) Clinical profile of congenital coronary artery anomalies with origin from the wrong aortic sinus leading to sudden death in young competitive athletes. J Am Coll Cardiol 35:1493–1501
3. Baltaxe HA, Wixson D (1977) The incidence of congenital anomalies of the coronary arteries in the adult population. Radiology 122:47–52
4. Datta J, White CS, Gilkeson RC, Meyer CA, Kansal S, Jani ML, Arildsen RC, Read K (2005) Anomalous coronary arteries in adults: depiction at multi-detector row CT angiography. Radiology 235:812–818
5. Saremi F, Abolhoda A, Ashikyan O, Milliken JC, Narula J, Gurudevan SV, Kaushal K, Raney A (2008) Arterial supply to sinuatrial and atrioventricular nodes: imaging with multidetector CT. Radiology 246:99–109
6. Saremi F, Channual S, Abolhoda A, Gurudevan SV, Narula J, Milliken JC (2008) MDCT of the S-shaped sinoatrial node artery. AJR Am J Roentgenol 190:1569–1575
7. Ortale JR, Paganoti Cde F, Marchiori GF (2006) Anatomical variations in the human sinuatrial nodal artery. Clinics 61:551–558
8. Pejković B, Krajnc I, Anderhuber F, Kosutić D (2008) Anatomical aspects of the arterial blood supply to the sinoatrial and atrioventricular nodes of the human heart. J Int Med Res 36:691–698
9. Ramanathan L, Shetty P, Nayak SR, Krishnamurthy A, Chettiar GK, Chockalingam A (2009) Origin of the sinoatrial and atrioventricular nodal arteries in South Indians: an angiographic study. Arq Bras Cardiol 92:314–319
10. Okmen AS, Okmen E (2009) Sinoatrial node artery arising from posterolateral branch of right coronary artery: definition by screening consecutive 1500 coronary angiographies. Anadolu Kardiyol Derg 9:481–485
11. Campbell JS (1929) Stereoscopic radiography of the coronary system. Quart J Med 22:247–268
12. Bokeriya LA, Mikhailin SI, Revishvili AS (1984) Anatomical variants of sinoatrial and atrioventricular node arteries. Cor Vasa 26:220–228
13. Caetano AG, Lopes AC (1995) Critical analysis of the clinical and surgical importance of the variations in the origin of sino-atrial node artery of the human heart. Rev Assoc Med Brass 41:94–102
14. Kawashima T, Sasaki H (2003) The morphological significance of the human sinoatrial nodal branch (artery). Heart Vessels 18:213–219
15. Mouchet A, Noureddine A (1926) Sur l'artère de l'atrionecteur. Ann Anat Pathol 1:41–48
16. Krupa U (1982) Studies on the coronary vascularization of atria of the heart. Folia Morphol (Warsz) 41:207–215
17. García-Villarreal OA, González-Oviedo R, Rodríguez-González H, Martínez-Chapa HD (2003) Superior septal approach for mitral valve surgery: a word of caution. Eur J Cardiothorac Surg 24:862–867
18. Busquet J, Fontan F, Anderson RH, Ho SY, Davies MJ (1984) The surgical significance of the atrial branches of the coronary arteries. Int J Cardiol 6:223–234
19. Kennel AJ, Titus JL (1972) The vasculature of human sinus node. Mayo Clin Proc 47:556–561
20. Raff GL, Gallagher MJ, O'Neill WW, Goldstein JA (2005) Diagnostic accuracy of noninvasive coronary angiography using 64-slice spiral computed tomography. J Am Coll Cardiol 46:552–557

21. James TN (1961) Anatomy of the human sinus node. Anat Rec 141:109–116
22. Romhilt DW, Hackel DB (1968) Origin of blood supply to sinoauricular and atrioventricular node. Am Heart J 75: 279–288
23. Hadziselimovic H (1978) Vascularization of the conducting system in the human heart. Acta Anat 102:105–110
24. Sow ML, Ndoye JM, Lô A (1996) The artery of the sinoatrial node: anatomic considerations based on 45 injection-dissections of the heart. Surg Radiol Anat 18: 103–109
25. Futami C, Tanuma K, Tanuma Y, Saito T (2003) The arterial blood supply of the conducting system in normal human hearts. Surg Radiol Anat 25:42–49
26. Vieweg WV, Alpert JS, Hagan AD (1975) Origin of the sinoatrial node and atrioventricular node arteries in right, mixed, and left inferior emphasis systems. Cathet Cardiovasc Diagn 1:361–373